

## Supplementary Information: Correlated Lateral and Vertical Transport of Large-Scale Majority Carrier Graphene-Insulator-Silicon Photodiodes

Hong-Ki Park, Yeonsoo Cho, Meongseop Kim, and Jaewu Choi \*

Quantum Information Display Laboratory, Department of Information Display, Kyung Hee University, 26, Kyungheedaero, Dongdaemun-gu, Seoul, 02447, Republic of Korea.

**Current-Voltage (I-V) Characteristic Analysis** Figure S1a and Figure S1b indicate I-V characteristic curves, which are observed at dark state at single and double electrode configurations, respectively. The I-V behaviors of graphene-insulator-silicon (GIS) heterostructures can be interpreted based on the modified Schottky diode equation with the lateral transport behavior as explained in the main manuscript (Equation 1) and here is re-expressed as below.<sup>1-4</sup>

$$I = WA * T^2 \exp(-\sqrt{\xi}d) \int_0^L \exp(-[\phi_s^e(V(x))/kT]) \{ \exp[q(V(x))/\eta^e kT] - 1 \} dx \quad (S1)$$

When the position dependent voltage variation is small, the following approximation can be assumed

$$\sqrt{V_a - IR_s - \Gamma x} = \sqrt{(V_a - IR_s) \left( 1 - \frac{\Gamma x}{V_a - IR_s} \right)} \cong \sqrt{V_a - IR_s} \left( 1 - \frac{\Gamma x}{2(V_a - IR_s)} \right) \because \left| \frac{\Gamma x}{(V_a - IR_s)} \right| \ll 1 \quad (S2)$$

Based on this, the integral equation for a single electrode configuration (Equation S1) can be expressed as

$$I_{1E}(0, 0.5) \cong WA * T^2 \exp(-\sqrt{\xi}d) \left\{ 4(V - IR_s) \left( qB_{ox}(\eta_0 + M \cdot V) \exp\left( \frac{(V - IR_s)}{(\eta_0 + M \cdot V)kT} \right) + (1 - qB_{ox}(\eta_0 + M \cdot V)) \exp\left( \frac{\Gamma x}{(\eta_0 + M \cdot V)kT} \right) \right) \right. \\ \dots (S3)$$

where 0 and 0.5 is the integration interval from 0 cm to 0.5 cm for junction length (L) in single electrode configuration. For the double electrode configuration, the integrated current equation can be expressed by

$$I_{2E} \cong 2I_{1E}(0, 0.25) \dots (S4)$$

In the case of the double electrode configuration, the current can be expressed based on the single electrode configuration as shown in Equation S3 while the integration is done over the half of channel length ( $L/2$ ). Using Equation (S3) and (S4), the experimental I-V curves for the single and double electrode configurations are fitted as shown in Figure S1a and Figure S1b, respectively.

The extracted physical parameters based on the fittings using Equation S3 and Equation S4 are confirmed by comparing the interface parameters obtained by Cheung's method based on the experimental  $J$ - $V$  characteristics at the relatively high forward bias voltage region (1.8 ~ 3V).<sup>5</sup> The first fitting plots (black circle) in Figure S1c and Figure S1d are  $d(V)/d(\ln J) = R_s A J + (q\eta^e/kT)$  versus  $J$  where  $J$  and  $A$  are current density ( $J=I/A$ ) and the junction area ( $A=WL$ ), respectively. A black dashed line of plotting  $d(V)/d(\ln J)$  versus  $J$  gives  $R_s$  and  $\eta^e$  from the slope and the y-intercept, respectively. The second plot (red square) is  $H(J) \equiv V - (\eta^e/\beta) \ln\{J/[A * T^2 \exp(\frac{q\phi_s^e}{kT}) (-\sqrt{\xi}d)]\} = R_s A J + \eta\phi_s^e$  versus  $J$ , which is also expressed from Schottky diode equation.  $R_s$  is also obtained from the slope and  $\phi_s^e$  is extracted from the y-intercept. Red squares and a red dashed line are experimental and fitting results, respectively. The extracted physical parameters from Cheung's method are indicated in Table 1.

**Dynamic response behaviors** At the single electrode configuration, Figure S2a and Figure S2b show the position dependent on-off photocurrent behaviors at 50 and 96  $\mu W$  optical power while Figure S2c and Figure S2d also show the position dependent on-off photocurrent behaviors for the double electrode configuration.

**Hot carrier effect by PMMA layer** Electrons having sufficient kinetic energy under a strong electrical field inside GIS junction devices can be directly injected into the PMMA layer from Si. As a result, the PMMA layer can be continuously charged under the bias voltages as well as the light illuminations as shown in Figure S3a.<sup>6</sup> When the illuminating light is off, the trapped carriers in the PMMA layer are gradually released to the graphene with time as shown in Figure S3b. When the PMMA layer is removed, the hot carrier charging effect was also removed as a previous report.<sup>3</sup>

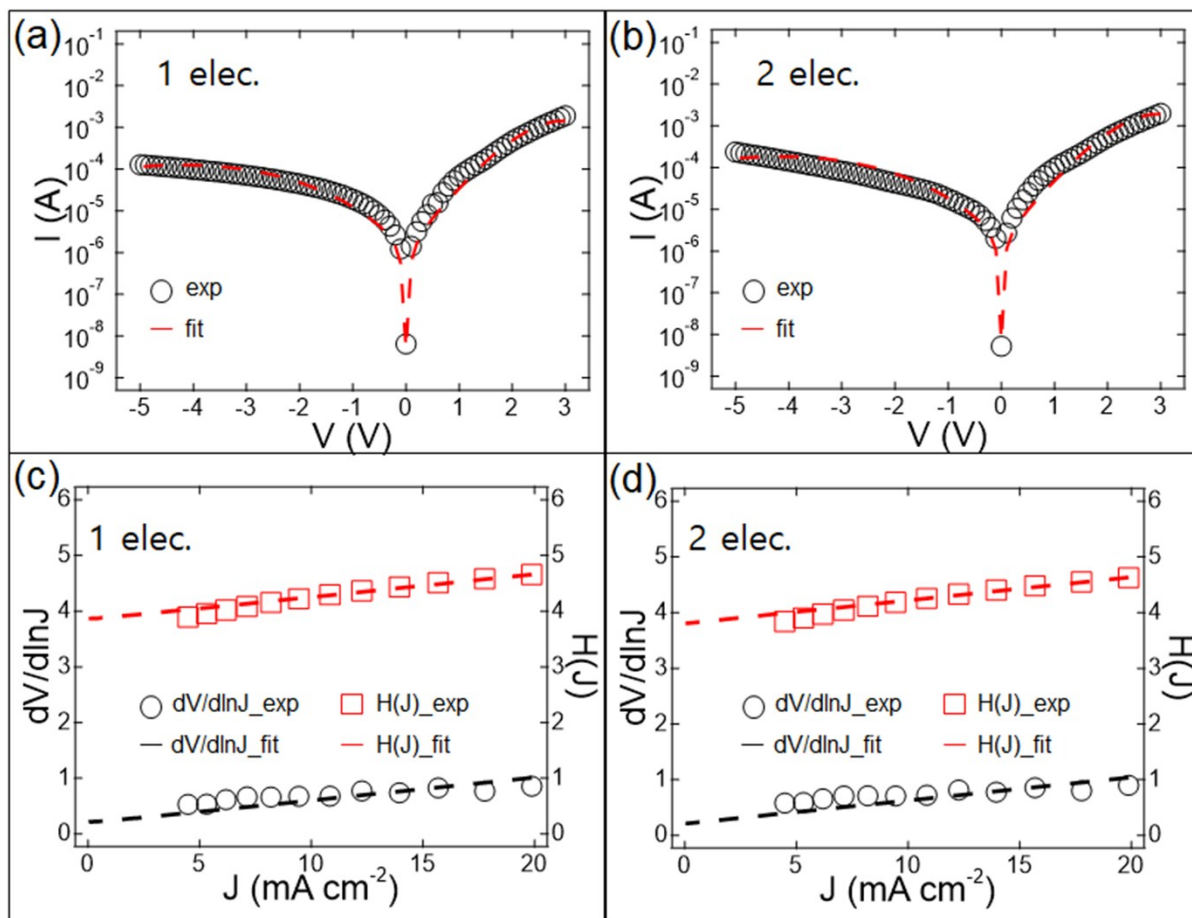


**Figure S1.** (a) and (b) Current-voltage (I-V) characteristics for the single and the double electrode configurations, respectively. The red dot lines show the fitted result obtained using Equation S2 and Equation S3, respectively. (c) and (d) The Cheung's plots of the I-V curves in forward bias voltage region ( $V=1.5\text{V}\sim 3\text{V}$ ). The fitted results based on the Cheung's method are shown by the dashed lines.

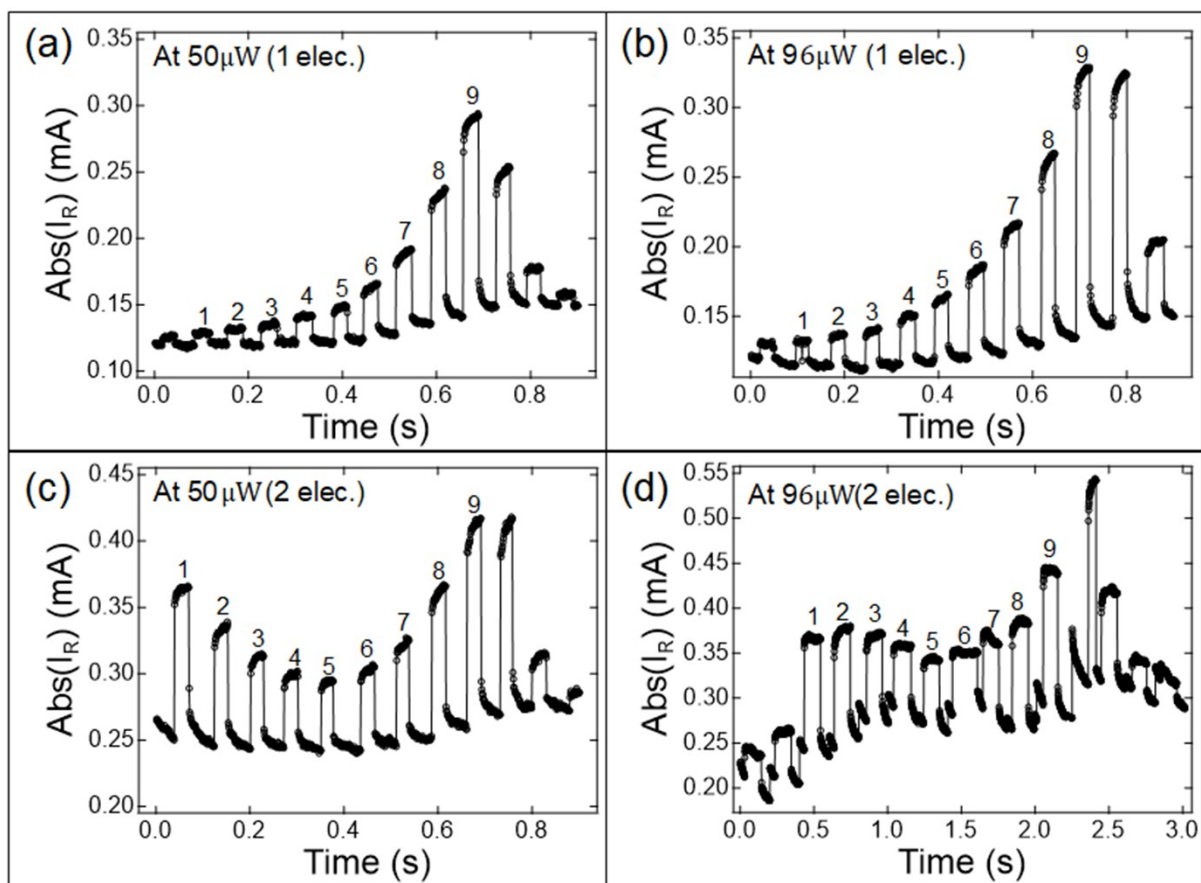


**Figure S2.** (a) and (b) The position dependent on-off photocurrent behaviors for the single electrode configuration under light illumination of the 50 and 96  $\mu W$ , respectively. (c) and (d) The position dependent on-off photocurrent behaviors for the double electrode configuration under light illumination of 50 and 96  $\mu W$ , respectively.

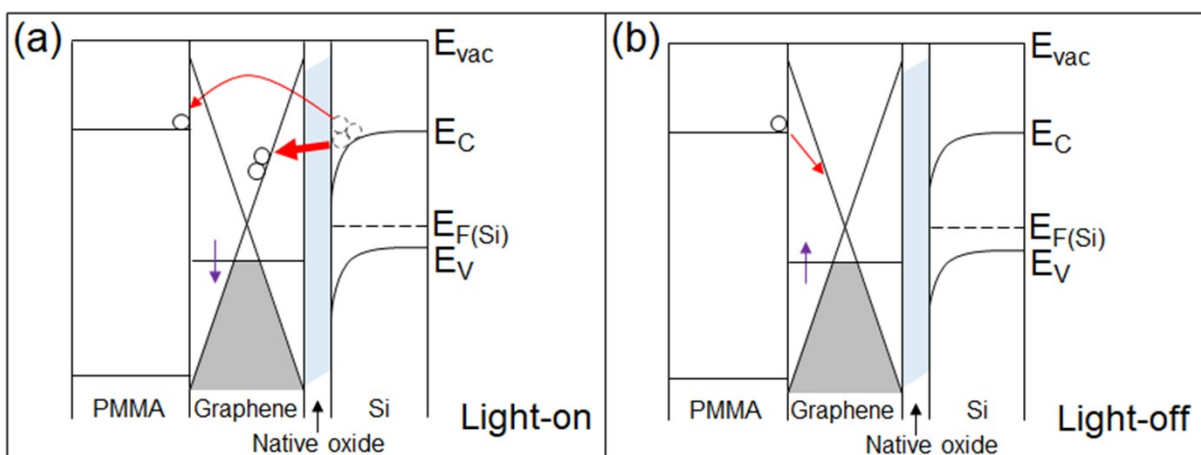


**Figure S3.** (a) and (b) Energy band diagrams for hot carrier injection in a GIS photodiode with a PMMA overlayer at a reverse bias voltage applied. (a) The hot carriers can be thermally generated in or photoexcited by light illumination in silicon and tunneled to the PMMA conduction band. (b) When the light is off, the captured hot carriers in the PMMA overlayer is gradually released to the graphene layer with time.

## References

- 1 H. K. Park, J. Choi *Adv. Electron. Mater.* 2018, **4**, 1700317.
- 2 H. K. Park, J. Choi *ACS Photonics* 2018, **5**, 2895-2903.
- 3 H. K. Park, J. Choi *J. Mater. Chem. C*, 2018, **6**, 6958-6965.
- 4 S. M. Sze and K. K. Ng, *Physics of Semiconductor Devices*, Wiley, Hoboken, NJ, USA, 2007.
- 5 S. K. Cheung and N. W. Cheung, *Appl. Phys. Lett.* 1986, **49**, 85.
- 6 H. Sun, Y. Cao, L. Feng, Y. Chen *Sci. Rep.* 2016, **6**, 1-10.